

Relaxation of Shot Peening Induced Residual Stresses in Ti-6Al-4V : Impact on Damage Tolerant Design

M. J. Shepard*

Air Force Research Laboratory, Materials and Manufacturing Directorate, Wright-Patterson AFB, OH, 45433-7817

Abstract

The Ti-6Al-4V components commonly found in turbine engines are frequently shot peened to induce compressive residual stresses in the near surface regions of these components. Due to uncertainty regarding the redistribution of residual stress fields in components during service and the difficulties associated with incorporating residual stresses in design, no design credit is typically taken for these compressive residual stresses.

In the current study, the redistribution of shot peening induced residual stresses, is reported for two common peening conditions, both before and after isothermal exposures. The importance of the different in-depth residual stress profiles arising from different peening conditions and isothermal exposures is explored in terms of a simple damage tolerant design.

It was found that useful compressive residual stresses persist well above the likely use temperature for this alloy. While it was found that substantial relaxation of shot peening induced residual stresses do occur, residual compressive stresses remain even after exposures as high as 200% of the expected use temperatures. These stresses are sufficient to yield substantial increases in damage tolerant design life.

Keywords: Fatigue, Fatigue Crack Growth, Residual Stress, Shot Peening, Stress Relaxation, Surface Treatments

1. Introduction

Shot peening is the most commonly used method for inducing compressive near surface residual stresses in turbine engine components. A detailed review of the shot peening process and its many applications is beyond the scope of this article. However many references are available and the reader is referred to those. [1,2]

It has long been observed that carefully called out, well controlled shot peening can yield many benefits including increased mean high cycle fatigue (HCF) performance, reduced scatter in HCF performance, and

* Corresponding author: michael.shepard@wpafb.af.mil Air Force Research Laboratory, 2230 Tenth St., Suite 1, WPAFB, OH 45433-7817

increased tolerance to small flaws. This increased damage tolerance is due to reduced stress intensity factor ranges induced by the shot peening induced compressive residual stresses.

Since many turbine engine components are designed using damage tolerant design practices, it is desirable to incorporate the lower fatigue crack growth (FCG) rates and higher threshold stress intensity factor ranges associated with shot peened surfaces into design practice. In theory, the former factor could allow for longer design lives and/or longer inspection intervals and the latter factor could allow for whether higher applied stresses with no predicted crack growth of slightly larger assumed flaws in the design. To date, the incorporation of these shot peening induced compressive residual stresses in design has been the exception rather than the rule. There are many reasons for this.

First, no widely accepted, nondestructive, subsurface residual stress analysis method exists that can measure the required residual stress profiles. Without such a method, it is impossible to verify that the subsurface residual stresses required for a given design are present in any given part. Second, it is not always certain that the desired shot peening residual stresses are always imparted in geometrically complex locations, such as radii and through holes. This is because these regions are not only difficult topeen, they are also the most challenging for residual stress analysis. Unfortunately, these locations are often the life limiting features since they act as stress concentrations. Third, even when there is often considerable confidence in the original residual stress profile due to tight quality control and representative residual stress analysis it is difficult to know if there has been any deleterious redistribution of the residual stresses due to thermal exposure and/or small amounts of inelastic deformation from overload induced plasticity or creep. Additionally, although the feasibility of incorporating known residual stresses in fracture mechanics calculations has been demonstrated by a number of authors [3,4,5,6] further experimental work is required to validate the current linear elastic fracture mechanics (LEFM) based approaches and develop more complex approaches that will be accurate in the complex multiaxial applied and residual stress states existing in real hardware. Finally, among many day-to-day users of shot peened components there is a general hesitancy to take design credit for these compressive stresses since they exist in such a physically thin region, which might be subject to redistribution due to handling damage or some other event.

The current study will not attempt to address all these admittedly non-trivial issues. Rather the current study will focus on the initial compressive residual stress profiles produced by common aerospace peening

conditions and how these profiles are altered by isothermal exposures. If these residual stresses are compromised excessively at the required operating temperatures, little design benefit will remain. The impact of these temperature induced stress redistributions on damage tolerant design life will be explored using LEFM calculations incorporating the modified residual stresses.

2. Experimental procedures

2.1 Specimen preparation

Small Ti-6Al-4V plates 63.5 mm square and 5 mm thick were machined from Ti-6Al-4V forged plate supplied by the National High Cycle Fatigue Program. The microstructural condition of these forgings is representative of that used in many turbine engine components. These plates were subjected to a vacuum stress relief anneal of 704 °C for 1 hour to relieve residual stresses associated with forging and machining.

These plates were then shot peened by Metal Improvement Company at the Blue Ash, Ohio facility. Half of the plates were peened to 6-9N Almen intensity with No. 5 glass beads. This peening condition is the lighter of the two studied conditions and is representative of a peening condition that might be used on an airfoil, where surface finish and edge tolerances are critical.

The remaining specimens were peened with S110 cast steel shot to 6-8A Almen intensity. This heavier peening condition commonly called out for use on Ti alloy hardware, such as in areas subjected to fretting fatigue, like dovetail slots or blade dovetails. This condition is known to induce deeper compression than the 6-9N condition, but the surface roughness associated with this condition can be substantial. (Roughened surfaces *can* be advantageous in certain settings, such as to aid in the adhesion of a plasma spray coating for fretting mitigation.) Coverage was fixed at 125% for both peening conditions.

Following peening each of the plates was sectioned with a water-cooled abrasive saw into 4 sub-coupons for subsequent thermal exposure and/or in-depth residual stress analysis.

Thermal exposures were conducted in lab air at temperatures of 250C, 325C, and 400C. For most turbine engine applications Ti-6Al-4V would not typically be used above about 200C, where its strength and stiffness are nominally 75% of their room temperature values. All thermal exposures were for 10 hours. Previous experiments exploring the thermal stability of surface treatment induced residual stresses in Ti and Ni based alloys as a function

of time at various temperatures have suggested that the majority of stress redistribution will occur inside relatively short times, likely less than 10 hours. [7]

2.2 X-ray diffraction residual stress and cold work measurement

X-ray diffraction residual stress measurements were made at the surface and at several depths below the peened surface. X-ray diffraction residual stress measurements were made employing a $\sin^2\psi$ technique and the diffraction of copper $K\alpha_1$ radiation from the (21.3) planes, of the Ti-6Al-4V. It was first verified that the lattice spacing was a linear function of $\sin^2\psi$, as required for the plane stress linear elastic residual stress model. [8,9,10,11]

Material was removed electrolytically for subsurface measurement in order to minimize possible alteration of the subsurface residual stress distribution as a result of material removal. The residual stress measurements were corrected for both the penetration of the radiation into the subsurface stress gradient [12] and for stress relaxation caused by layer removal. [13]

The value of the x-ray elastic constants required to calculate the macroscopic residual stress from the strain normal to the (21.3) planes of the Ti-6Al-4V were determined in accordance with ASTM E1426-91. [14] Systematic errors were monitored per ASTM specification E915.

2.3 Linear Elastic Fracture Mechanics Methods

Estimates of propagation life for assumed flaws embedded in experimentally determined residual stress fields were made using the linear elastic fracture mechanics software package AFGROW, which was developed by the U.S. Air Force. The calculations used an approximate K solution developed by Wang [15] for a surface flaw subjected to an arbitrary stress field based on the weight function method as proposed by Shen and Glinka. [16] Initial inputs for this model were as follows: an initial semi-elliptical surface flaw, $a = c = 0.508\text{mm}$ in Ti-6Al-4V plate $t = 100\text{ mm}$, $w = 400\text{ mm}$. The assumed residual stresses for the baseline peening conditions were averaged from the three replications of each peening condition. Residual stress distributions for post-isothermal exposure predictions were taken from single replicates. All predictions are for stress ratio $R = 0.1$. Life predictions do not include any correction for plasticity-induced crack retardation or crack initiation. Design guidance for turbine engine components suggests “infinite” life components such as fan blades should be designed to a life of 10^7 fatigue cycles, thus crack growth predictions were terminated at this point.

Crack growth predictions were terminated at 10^7 cycles, which is consistent with the fatigue databases used in most turbine engine designs.

The author recognizes the limitations of the methods described above. However, since the intent of the current study is only to explore the potential for using shot peening induced stresses importance of modest changes in peening induced stress distributions on damage tolerant life, the above methods are viewed as being adequate to estimate the order of magnitude of peening induced crack growth retardation and the impact of isothermal exposures.

3. Results and discussion

3.1 As peened residual stresses

The residual stress distributions measured as functions of depth are shown graphically in Figures 1 and 2 for the 6-9N and 6-8A intensity peening conditions respectively. Compressive stresses are reported as negative values and tensile stresses as positive values. Trend lines represent a cubic spline curve fit to the data and are intended as a visual aid only. Three replications were made for each of the peening conditions to ascertain what level of variability might be encountered in the residual stresses induced by these peening configurations due to small variations in the peening process and material response.

Additional surface only measurements were made on other coupons prior to their assigned isothermal exposures to further investigate the variability in the peening induced stress states. These results are reported in table 1. These surface only measurements are “raw” values and are not corrected for the penetration of the x-rays into the stress gradient existing in the specimen. Precise corrections are not possible for surface only measurements, since the existing stress gradient cannot be quantified without subsurface measurements.

The surface stresses induced by both the 6-9N and 6-8A peening conditions were extremely repeatable across all observations. In fact, based on the observations tabulated in Table 1 it can be concluded that the surface residual stresses associated with the 6-9N and 6-8A peening conditions are statistically identical. The ramifications of this finding will be further explored in section 3.3.

There were noticeable differences in the in-depth residual stresses observed among the different replications of the two peening conditions. (Figures 1 and 2) With only three replicates available per condition, it

is not possible to place statistical bounds on the limits of the in-depth residual stresses. For an academic exercise it is sufficient to simply average the available data. (Figure 3) In a design environment, however, it would be necessary to have a statistical understanding of the lower bound of the imparted residual stresses so that this more conservative estimate of the stresses could be used in the design.

The subsurface residual stresses produced by the two different peening conditions differed substantially in the depth of compression induced. An averaged residual stress profile from each of the peening conditions is depicted in Figure 3. It can be seen that the compressive stresses induced by the more intense 6-8A peening condition are on the order of twice as deep at 0.15mm deep versus those induced by the less intense 6-9N peening condition, at 0.07mm deep.

3.2 Residual stresses after isothermal exposure

Figures 4 and 5 depict in-depth residual stress profiles after isothermal exposures for the 6-9N GBP and the 6-8A SP conditions respectively, compared to an unexposed average residual stress profile using the same peening conditions. While it can be seen that substantial redistribution of the stresses occurs, surface compression remains even after exposures as high as 400C, which is on the order of 200% of the maximum expected use temperature. Further, the magnitude of the residual compression after isothermal exposures at 250C remains relatively high, suggesting that there will be substantial design life benefits in damage tolerant designs incorporating these residual compressive stresses.

It is believed that the redistribution of the residual stresses reported here is due to two sets of factors. Firstly, as temperature increases the modulus and yield strength of the Ti-6Al-4V will drop substantially. The yield surface changes and stresses that were previously accommodated within the bounds of elasticity become plastic, leading to redistribution of the stress state. This element of the redistribution behavior is not time dependant and will occur nearly real-time as the specimen is subjected to thermal excursions.

The second factor is creep. Although, the temperatures in this experiment are not particularly high in terms of homologous temperature, the stresses are very high as a percentage of yield strength. As a result, creep strain is expected to add a time dependent component to the redistribution behavior. The impact of primary creep should be well represented in the current experiments, but the longer term impact of secondary creep is not well

captured by the current experiments. As discussed earlier in section 2.1, it is expected that the impact of longer-term (creep driven) redistribution is smaller than the effects of shorter-term mechanisms.

Optimally, future work would include longer-term exposures as well as mean loads, since both of these factors will be present in any turbine engine application.

3.3 Life Predictions

Predictions for propagation life for the baseline unpeened, average 6-8A shot peened, and 6-8A shot peened plus isothermal exposure conditions are plotted in Figure 6. The positive impact of the shot peening induced residual stresses on fatigue crack growth, and thus propagation life, is apparent in both the finite life and high cycle fatigue regimes. In the finite life regime, where the maximum applied stresses are limited by yield strength (~830 MPa) the life benefit is approximately 6X before isothermal exposure. Even after isothermal exposure at 400C, greater than 200% of the anticipated max use temperature, a small predicted benefit persists in this regime.

In the lower applied stress, longer life regime the benefits of the shot peening induced residual stresses are also very apparent. In this regime, the compressive stresses act not just to slow fatigue crack growth, but to keep the total stress intensity factor range below the threshold level, thus preventing crack growth and ensuring essentially infinite predicted lives. Even after the most severe isothermal exposure, sufficient peening induced compressive residual stresses remain to prevent significant crack growth at stresses on the order of times higher than those in the similarly loaded unpeened case.

Similar trends to those found in the 6-8A peening conditions are found in the 6-9N glass bead peening predictions found in figure 7. The magnitude of the benefit, however, is more modest compared to the 6-8A shot peened condition due to the more shallow induced compression with glass bead peening. Again, in both the short and long life regimes, significant propagation life benefits are predicted even after the most severe isothermal exposure.

4. Conclusions

Ti-6Al-4V plates were shot peened to two common aerospace peening conditions and then subjected to in-depth x-ray diffraction residual stress analysis after different isothermal exposures. It has been found that substantial compressive residual stresses due to shot peening can persist in Ti-6Al-4V after isothermal exposures well exceeding expected use temperatures.

The impact of this residual stress redistribution was explored in terms of a simple linear elastic fracture mechanics model. The analysis suggests a substantial increase in propagation life over an unpeened baseline condition for both the 6-8A shot peened and 6-9N glass bead peened conditions, with the higher intensity 6-8A condition being superior. Even after aggressive isothermal exposures both peening conditions retained sufficient compressive residual stresses to positively impact propagation life versus the baseline condition.

Tables

Table I

Trial	Surface Stresses By Peening Condition (MPa)	
	6-9N Glass Bead Peened	6-8A Shot Peened
1	-714	-717
2	-703	-714
3	-697	-710
4	-706	-752
5	-676	-690
6	-679	-708
AVERAGE	-696	-715

Figures

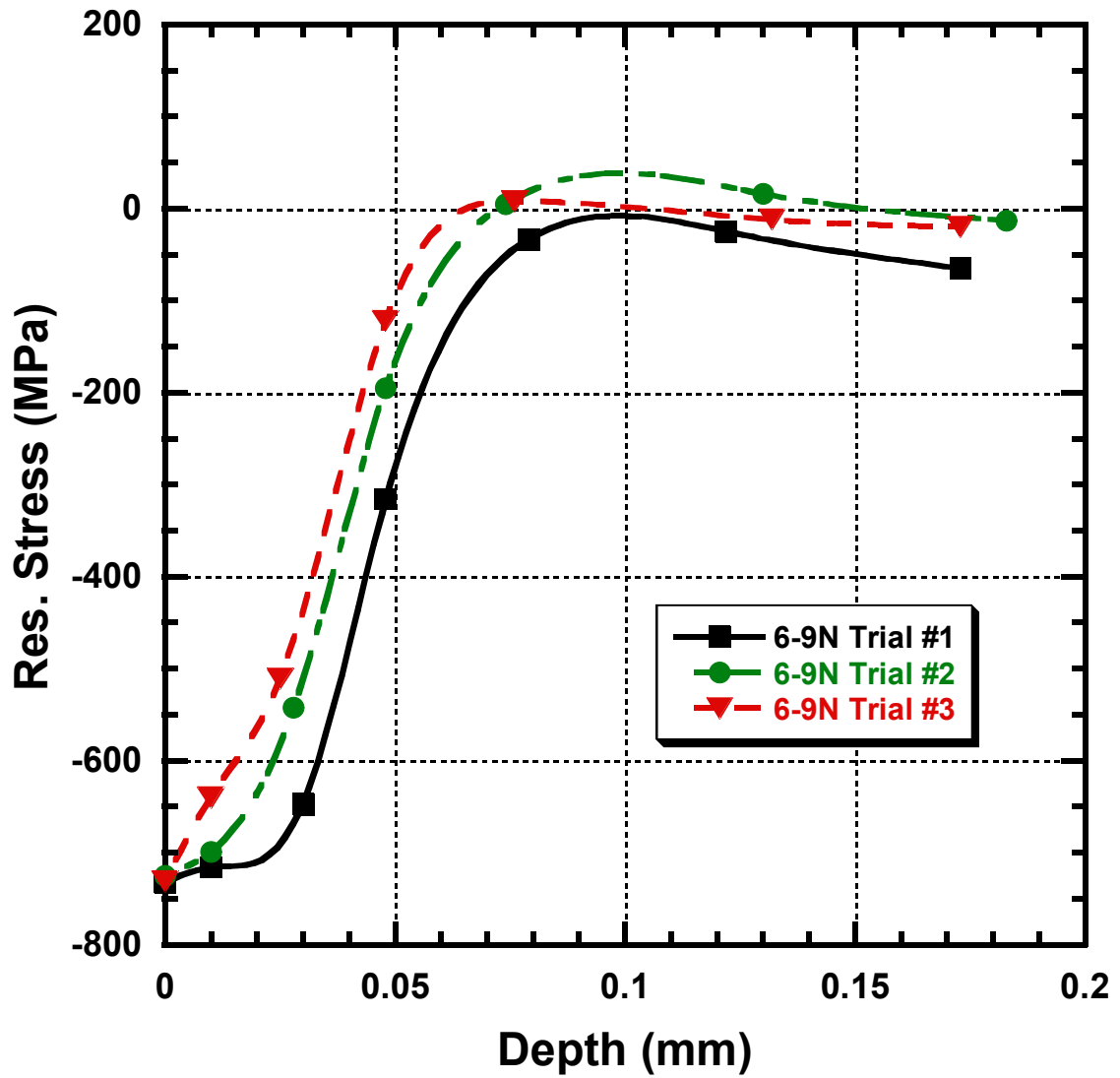


Figure 1: In-depth residual stresses from 3 replications of 6-9N glass bead peening

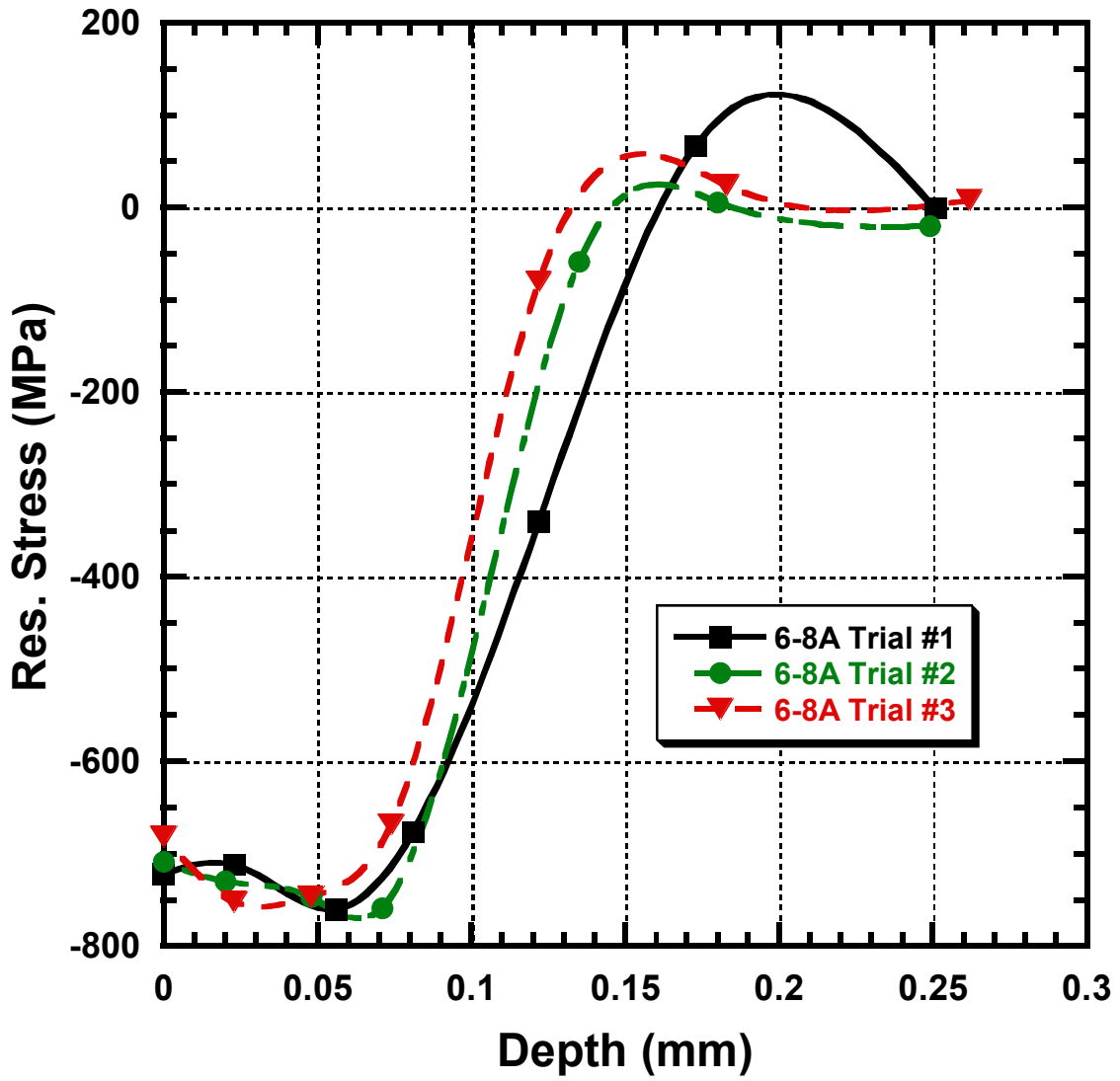


Figure 2: In-depth residual stresses from 3 replications of 6-8A shot peening

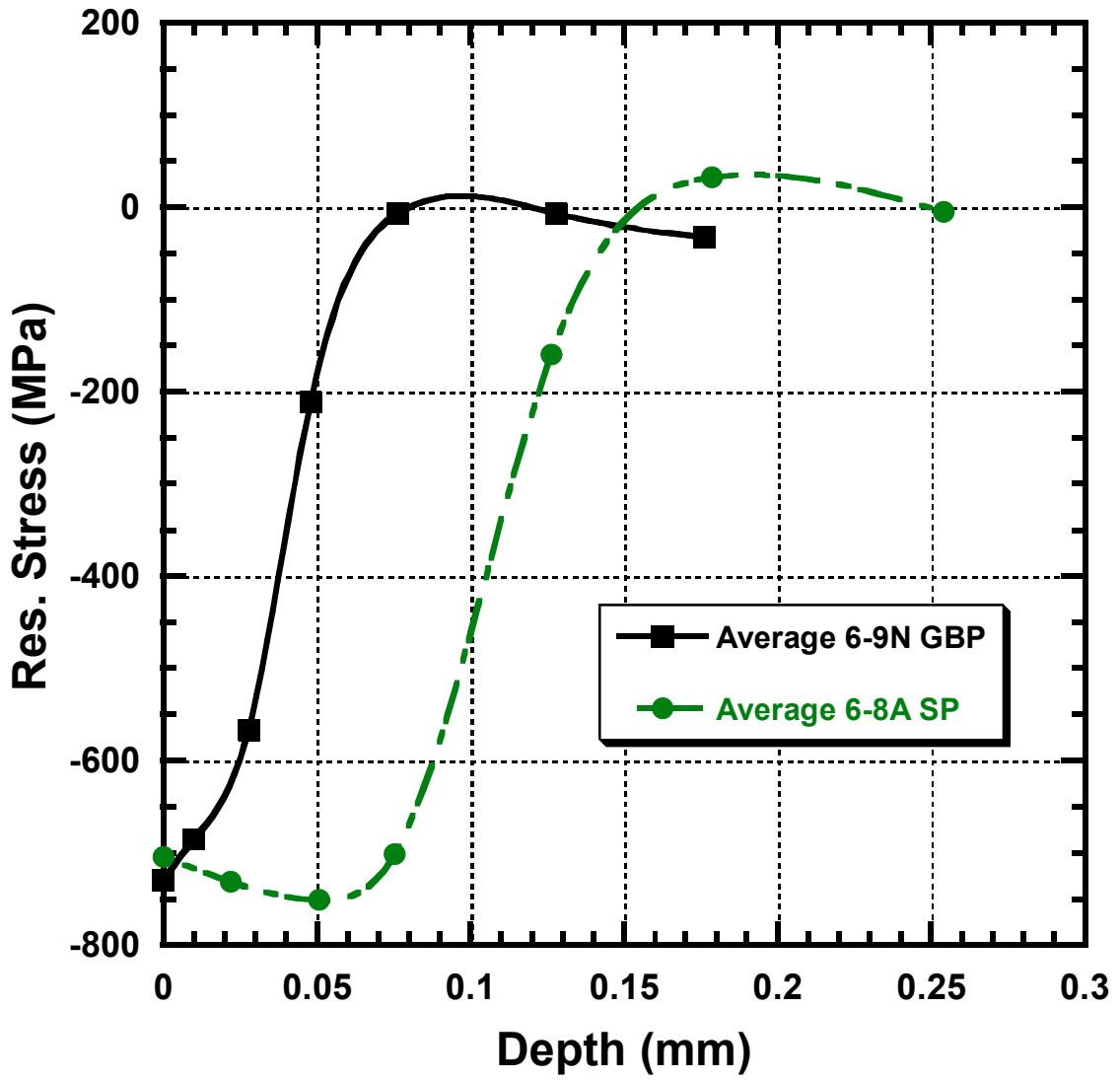


Figure 3: In-depth residual stress comparison, average 6-9N intensity vs. average 6-8A intensity

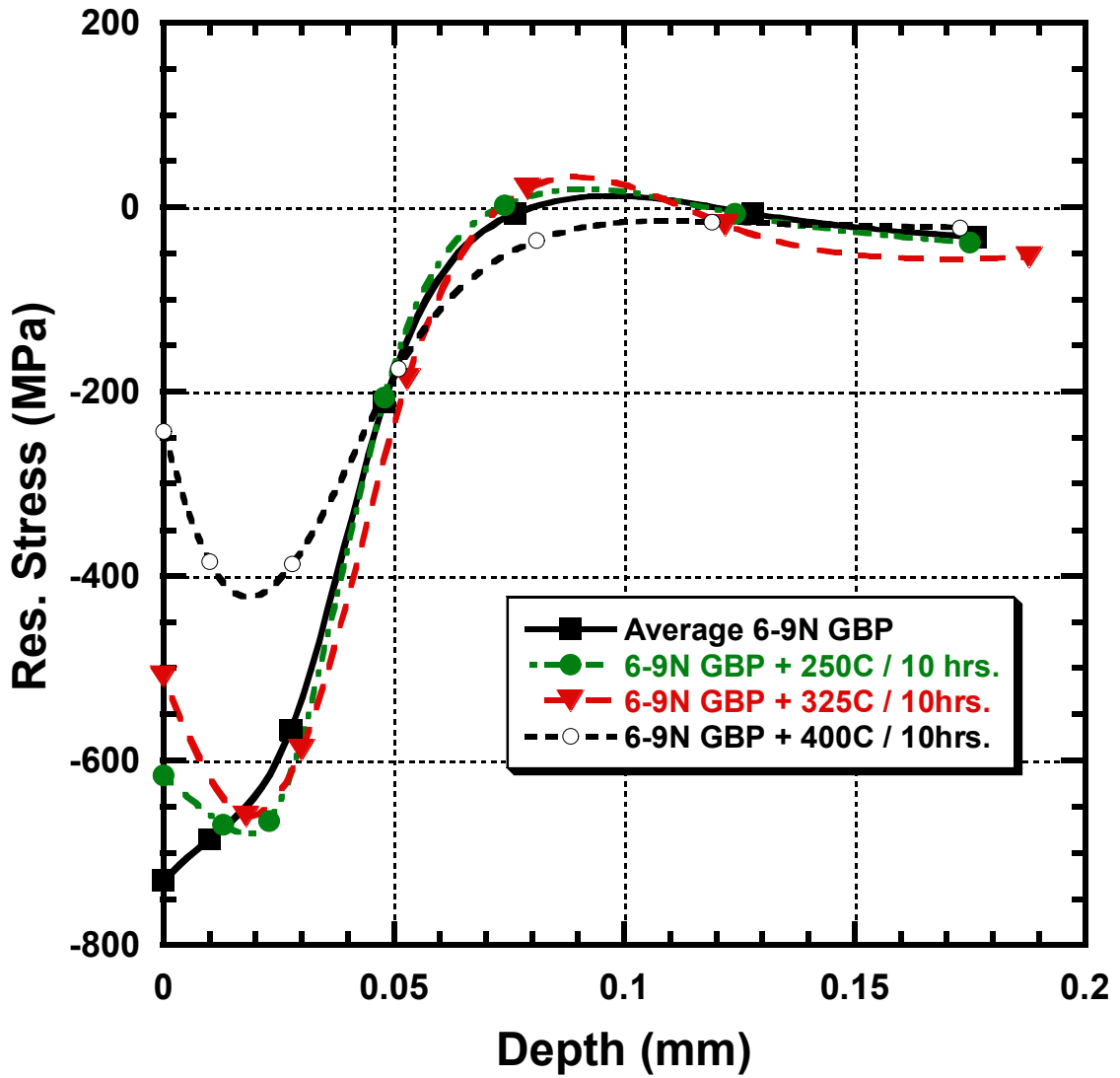


Figure 4: In-depth residual stresses for the 6-9N GBP condition before and after isothermal exposure

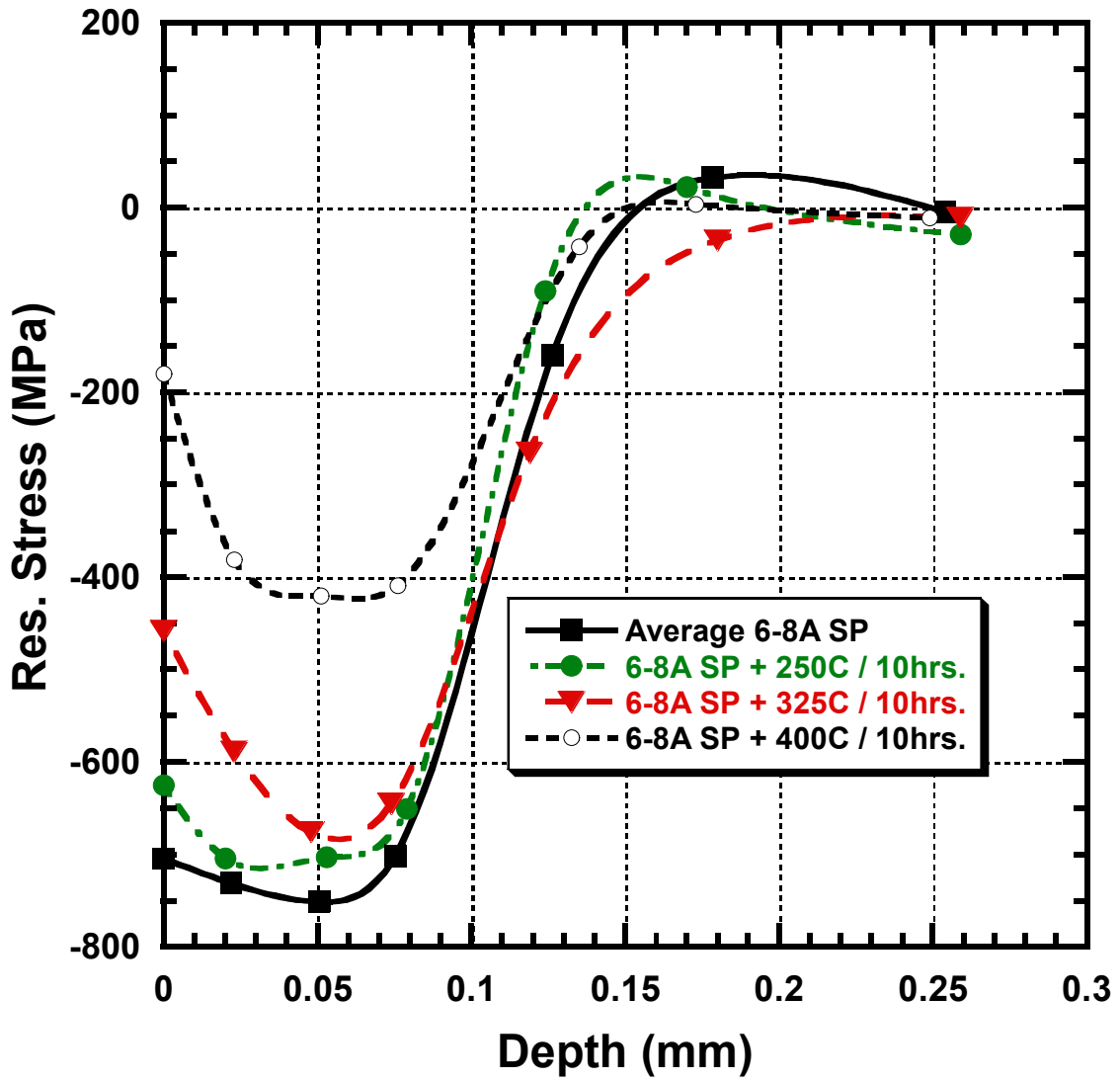


Figure 5: In-depth residual stresses for the 6-8A SP condition before and after isothermal exposure

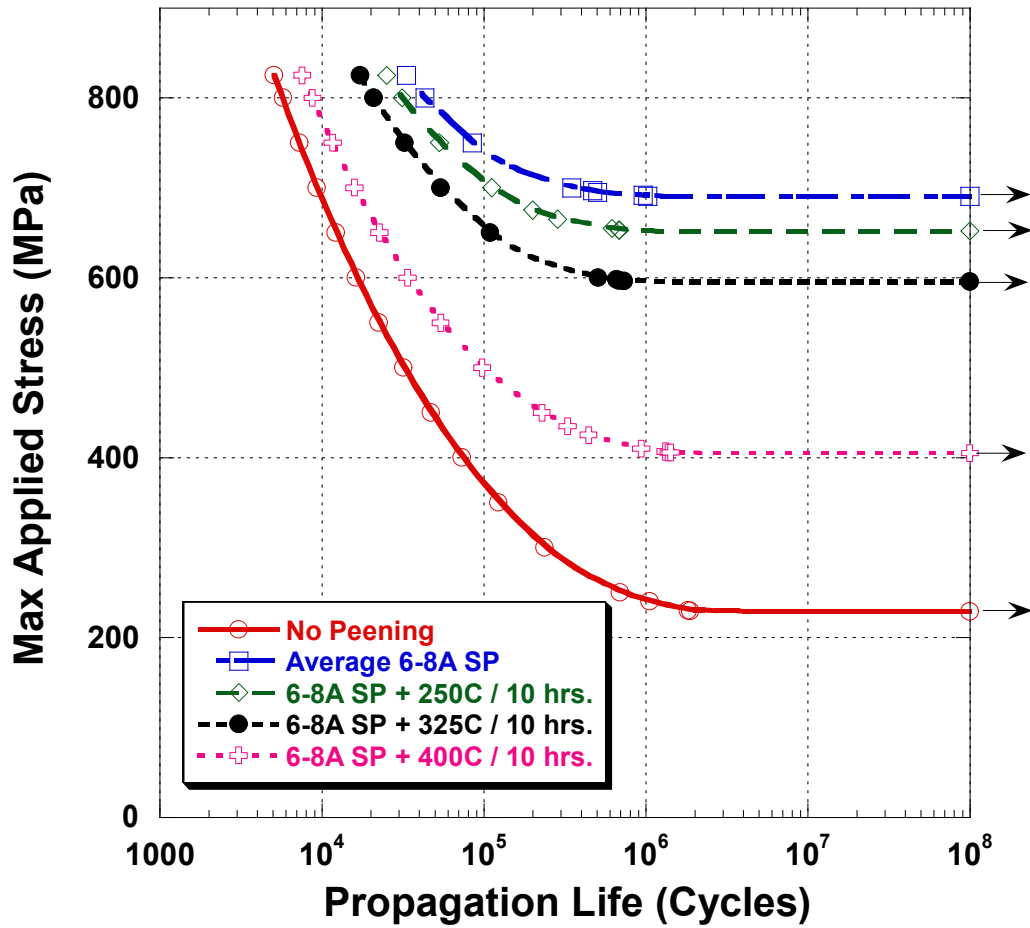


Figure 6: LEFM Predictions for Ti-6Al-4V baseline, 6-8A shot peened, and 6-8A shot peened+ isothermal exposure. (Semi-elliptical surface flaw $a = c = 0.508\text{mm}$ in Ti-6Al-4V plate $t = 100\text{ mm}$, $w = 400\text{ mm}$.)

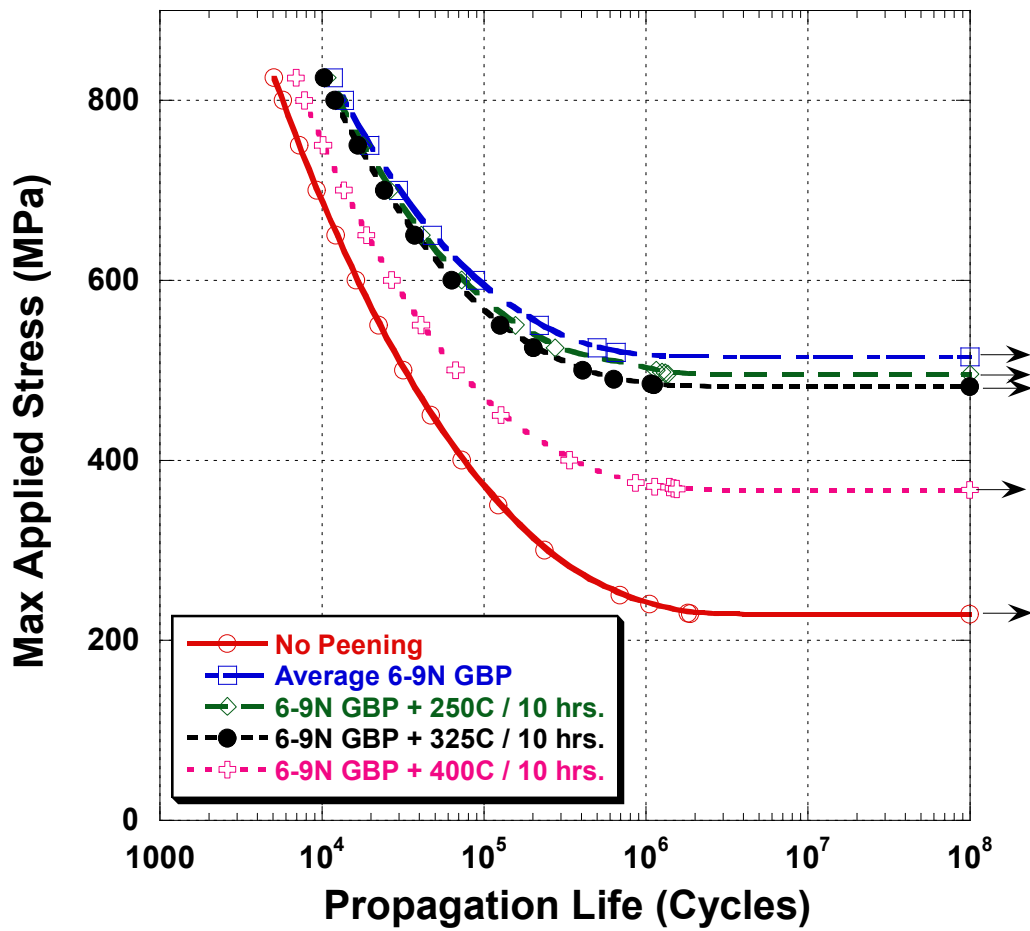


Figure 7: LEFM Predictions for Ti-6Al-4V baseline, 6-9N glass bead peened, and 6-9N glass bead peened + isothermal exposure. (Semi-elliptical surface flaw $a = c = 0.508\text{mm}$ in Ti-6Al-4V plate $t = 100\text{ mm}$, $w = 400\text{ mm}$.)

References:

1. Niku-Lari, A. (1981). Shot-Peening. First International Conference on Shot Peening, Paris, France, Out of Print: Full Text Available at <http://www.shotpeening.org/>.
2. Al-Hassani, S. T. S. (1982). The Shot Peening of Metals - Mechanics and Structures. Aerospace Congress and Exposition, Anaheim, CA, Society of Automotive Engineers, Inc., 400 Commonwealth Dr., Warrendale, PA 15096.
3. Glinka, G. (1979). Effect of Residual Stresses on Fatigue Crack Growth in Steel Weldments Under Constant and Variable Amplitude Loads. Fracture Mechanics, ASTM STP 677. C. W. Smith, American Society for Testing and Materials: 198-214.
4. Kang, H. J., Song, J. H., Earmme, Y. Y. (1989). "Fatigue Crack Growth and Closure Through A Tensile Residual Stress Field Under Compressive Applied Loading." Fatigue Fract. Engng Mater. Struct. **12**(5): 363-376.
5. Beghini, M., Bertini, L. (1990). "Fatigue Crack Propagation Through Residual Stress Fields with Closure Phenomena." Engineering Fracture Mechanics **36**(3): 379-387.
6. Beghini, M., Bertini, L., Vitale, E. (1994). "Fatigue Crack Growth in Residual Stress Fields: Experimental Results and Modeling." Fatigue Fract. Engng Mater. Struct. **17**(12): 1433-1444.
7. P. Prev y, D. H., P. Mason (1997). Thermal Residual Stress Relaxation and Distortion in Surface Enhanced Gas Turbine Components. ASM/TMS Materials Week, Indianapolis, IN.
8. Residual Stress Measurement by X-Ray Diffraction, *SAE J784a*. Hilley, M.E. ed. (1971), Warrendale, PA: Society of Auto. Eng.
9. Noyan, I. C. and J. B. Cohen. Residual Stress Measurement by Diffraction and Interpretation, New York, NY: Springer-Verlag, 1987.
10. Cullity, B. D. Elements of X-ray Diffraction, 2nd ed. Reading, MA: Addison-Wesley, 1978, pp. 447-476.
11. Prev y, P. S., "X-Ray Diffraction Residual Stress Techniques," *Metals Handbook*, **10**, (Metals Park, OH: ASM, 1986, pp 380-392.
12. Koistinen, D. P. and Marburger, R. E., (1964), Transactions of the ASM, **67**.

13. Moore, M. G. and Evans, W. P., (1958) "Mathematical Correction for Stress in Removed Layers in X-Ray Diffraction Residual Stress Analysis," SAE Transactions, **66**, pp. 340-345
14. Prev y, P. S., (1977), "A Method of Determining Elastic Properties of Alloys in Selected Crystallographic Directions for X-Ray Diffraction Residual Stress Measurement," Adv. In X-Ray Analysis, **20**, (New York, NY: Plenum Press, 1977), pp 345-354.
15. Boyd, K. L., S. Krishnan, et al. (1997). Development of Structural Integrity Analysis Technologies for Aging Aircraft Structures: Bonded Composite Patch Repair and Weight Function Methods. WPAFB, OH, Flight Dynamics Directorate, Wright Laboratory, AFMC: 133.

or

Wang, X. "Weight Functions for High Aspect Ratio Semielliptical Surface Cracks in Finite-Thickness Plates," University of Waterloo, to be published.
16. Glinka, G. and G. Shen (1991). "Universal Features of Weight Functions for Cracks in Mode I." Engineering Fracture Mechanics **40**(6): 1135-1146.